Synthesis and Photovoltaic Properties of a D–A Copolymer Based on the 2,3-Di(5-hexylthiophen-2-yl)quinoxaline Acceptor Unit

Kun Wang, Zhi-Guo Zhang, Qiang Fu,* Yongfang Li*

A new D–A copolymer (**PBDT-DTQx**) based on the 2,3-di(5-hexylthiophen-2-yl)quinoxaline acceptor unit and a bithienyl-substituted benzodithiophene (BDT) donor unit is designed and synthesized for application as the donor material in polymer solar cells (PSCs). The polymer film shows a broad absorption band covering the wavelength range from 300 to 720 nm and a low highest occupied molecular orbital (HOMO) energy level at −5.35 eV. A device based on **PBDT-DTQx**:$PC_{70}BM$ ([6,6]-phenyl-C71-butyric acid methyl ester) (1:2.5, w/w) with chloronaphthalene as a solvent additive displays a power conversion efficiency (PCE) of 3.15%. With methanol treatment, the PCE of the PSCs is further improved to 3.90% with a significant increase of the short-circuit current density, J_{sc}, from 10.10 mA cm^{-2} for the device without the methanol treatment to 11.71 mA cm^{-2} for the device with the methanol treatment.

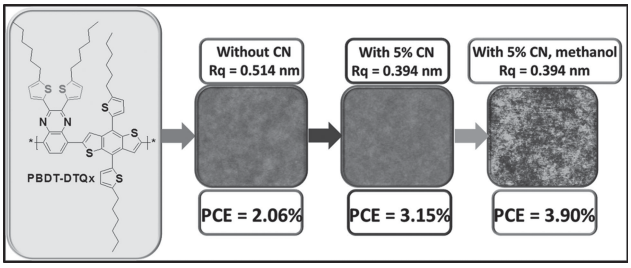

1. Introduction

Bulk-heterojunction (BHJ) polymer solar cells (PSCs)[1] have developed quickly in recent years. Power conversion efficiencies (PCE) higher than 8%[2–4] have been achieved by synthesizing new photovoltaic materials and fabricating new device structures.[5,6]

In the development of new conjugated polymer donor materials, various D–A copolymers of a donor unit (D) and an acceptor unit (A) were designed and synthesized, and many of them show promising photovoltaic properties. It is crucial to understand the relationship between molecular structure and device performance.[7] The choice of the donor (D) and acceptor (A) units directly determines the nature of the D–A copolymers and the performance of the PSCs with the polymer as donor material. Among various electron-donor units, benzo[1,2-b:4,5-b′]dithiophene (BDT) has attracted great attention due to its symmetric and planar conjugated structure, and good photovoltaic performance of the copolymers containing BDT-donor unit.[8]

Quinoxaline (**Qx**)[9–12] is a typical electron-deficient unit with strong electronegativity due to the two nitrogen atoms in it. A high photovoltaic performance has been reported for D–A copolymers containing the **Qx**-acceptor unit.[13] In addition, it is reported that the substituent on **Qx** has a great influence on the optical properties, molecular energy levels, and photovoltaic performance of the corresponding copolymers.[10–12] 2,3-Diphenylquinoxaline, which possesses two separated phenyl rings, is one of the commonly investigated **Qx** derivatives because of its facile synthesis and versatility.[12,13] However, the copolymers based on 2,3-di(thiophen-2-yl) quinoxaline-acceptor unit, which is the thiophene substituent on **Qx**, was seldom reported.[14]

Here, we report a new alternating D–A copolymer with BDT as donor unit and 2,3-di(5-hexylthiophen-2-yl)

K. Wang, Dr. Z.-G. Zhang, Prof. Y. Li
Beijing National Laboratory for Molecular Sciences, CAS Key Laboratory of Organic Solids, Institute of Chemistry Chinese Academy of Sciences, Beijing 100190, China
E-mail: liyf@iccas.ac.cn
Prof. Q. Fu
Faculty of Chemistry, Northeast Normal University Changchun 130024, China
E-mail: fqiang@nenu.edu.cn

DOI: 10.1002/macp.201300793

quinoxaline (**DTQx**) as acceptor unit, **PBDT-DTQx**, for the application as donor materials in PSCs. The effect of the thiophene side chain on the electronic energy level and photovoltaic performance of the polymer was studied in detail.

2. Experimental Section

2.1. Materials

The monomers 1,4-dibromo-2,3-diaminobenzene[9b,15] 1,2-bis(5-hexylthiophen-2-yl)ethane-1,2-dione (**a**),[15,16] and 5,8-dibromo-2,3-bis(5-hexylthiophen-2-yl)quinoxaline ($\mathbf{A_1}$)[9b,15] were prepared according to the method reported in the literature. Solvents (tetrahydrofuran (THF), *N*,*N*-dimethylformamide (DMF), and toluene) were dried by standard procedure and distilled before use. All of the other chemicals were purchased from Alfa Aesar and used without further purification.

2.2. Measurements and Instrumentation

^{1}H NMR and ^{13}C NMR spectra were measured on a Bruker DMX-400 spectrometer with *d*-chloroform as the solvent and tetramethylsilane as the internal reference. UV–visible absorption spectra were measured on a Hitachi U-3010 UV–vis spectrophotometer. Mass spectra were recorded on a Shimadzu spectrometer. Thermogravimetric analysis (TGA) was conducted on a Perkin–Elmer TGA-7 thermogravimetric analyzer at a heating rate of 20 °C min^{-1} and under a nitrogen flow rate of 100 mL min^{-1}. Gel permeation chromatography (GPC) measurements were conducted, using polystyrene as standard and THF as the eluent. The electrochemical cyclic voltammetry was conducted on a Zahner IM6e Electrochemical Workstation, in a 0.1 mol L^{-1} acetonitrile solution of tetrabutylammonium hexafluorophosphate (n-Bu_4NPF_6) at a potential scan rate of 100 mV s^{-1} with a Ag/AgCl reference electrode and a platinum wire counter electrode. Polymer film was formed by drop-casting 1.0 μL of polymer solutions in THF (analytical reagent, 1 mg mL^{-1}) onto the working electrode, and then dried in the air. The film morphology was measured using an atomic force microscope (SPA-400) using the tapping mode.

2.3. Device Fabrication and Characterization of PSCs

The PSCs were fabricated with a configuration of indium tin oxide (ITO)/poly(3,4-ethylenedioxythiophene):poly(styrenesulfonate) (PEDOT:PSS) (40 nm)/active layer/Ca (20 nm)/Al (100 nm). A thin layer of PEDOT:PSS was spin-cast on pre-cleaned ITO-coated glass from a PEDOT:PSS aqueous solution (Baytron P VP AI 4083 from H. C. Starck) at 3000 rpm and thermal-treated at 150 °C for 10 min; then, the electrode was transferred to a glove box. In the glove box, the active layer of the blend of the polymer donor and PCBM ([6,6]-phenyl-C61-butyric acid methyl ester ($PC_{60}BM$) and [6,6]-phenyl-C71-butyric acid methyl ester ($PC_{70}BM$)) acceptor was spin-coated onto the PEDOT:PSS layer from a *o*-dichlorobenzene (*o*-DCB) solution of the donor and acceptor, chloronaphthalene (CN) or 1,8-diiodooctane (DIO) was used as processing additive to optimize the morphology, and pre-thermal annealing at 120 °C for 10 min was performed before deposition of the metal-top electrode. Finally, a Ca/Al metal-top electrode was deposited in vacuum onto the active layer at a pressure of ca. 5×10^{-5} Pa. The active area of the device was 4 mm^2. The thickness of the active layer was determined using an Ambios Tech. XP-2 profilometer. The current density–voltage (*J*–*V*) characteristics were measured on a computer-controlled Keithley 236 Source-Measure Unit. A xenon lamp coupled with an AM 1.5 solar spectrum filter was used as the light source, and the optical power at the sample was 100 mW cm^{-2}.

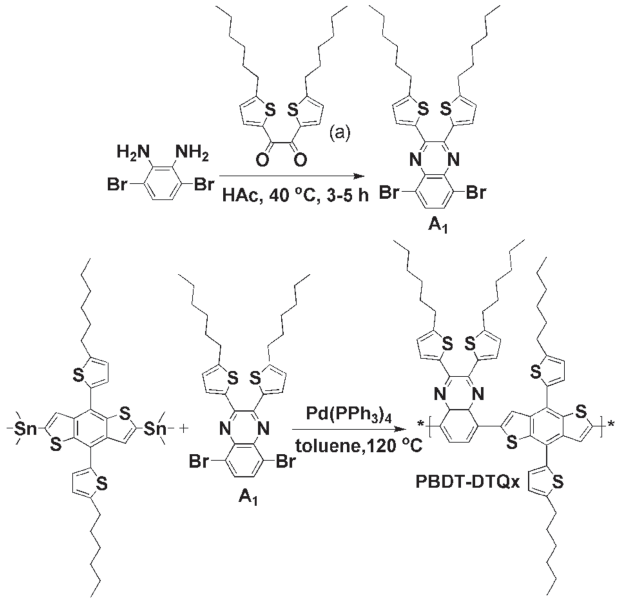

Scheme 1. Synthetic route for the monomer $\mathbf{A_1}$ and the polymer **PBDT-DTQx**.

2.4. Synthesis of Monomers and Copolymer

Molecular structures and synthesis routes of monomers and the copolymer are shown in Scheme 1. The detailed synthetic processes are as follows.

2.5. Synthesis of Monomers

2.5.1. 1,2-Bis(5-hexylthiophen-2-yl)ethane-1,2-dione (a)[15]

A solution of LiBr (4.67 g, 53.8 mmol) in tetrahydrofuran (THF), (20 mL) was added to a suspension of CuBr (3.86 g, 36.9 mmol) in THF (100 mL). The mixture was stirred at room temperature until it became homogeneous and was then cooled to 0 °C in an ice-water bath. To this was added a Grignard reagent that was prepared by dropwise addition of a solution of 2-bromo-5-hexylthiophene (6.65 g, 26.9 mmol) in THF (10 mL) to a suspension of magnesium (Mg) (0.89 g, 37.1 mmol) in THF (20 mL). After 10 min, oxalyl chloride (1.52 g, 12 mmol) was added and the mixture was stirred at 0 °C for 20 min and was quenched with saturated NH_4Cl. It was then extracted with ethyl acetate and the combined extract was washed with brine, dried over Na_2SO_4, and the solvent was removed, which was subsequently

chromatographed over silica gel using petroleum ether as eluent to afford yellow solid compound (3.42 g, 73%). ^{1}H NMR ($CDCl_3$, 400 MHz, δ): 7.19 (d, 2H), 6.80 (d, 2H), 2.56 (t, 4H), 1.59 (m, 6H), 1.36–1.31 (m, 10H), 0.89 (m, 6 H). ^{1}H NMR spectra of the compounds **a** with the assignment of the NMR signals are given in Figure S1 (Supporting Information). GC/MS *m/z*: $[M]^+$ calcd for $C_{22}H_{30}O_2S_2$, 390; found, 390, 195.

2.5.2. 5,8-Dibromo-2,3-bis(5-hexylthiophen-2-yl) quinoxaline (A_1)

A mixture of compound 1,4-dibromo-2,3-diaminobenzene (1.13 g, 5 mmol), compound **a** (1.95 g, 5 mmol), and acetic acid (70 mL) was briefly warmed to 40 °C, and the solution was then stirred at room temperature for 3 h. The precipitate was collected by filtration, washed with ethanol, and dried to afford bright yellow solid $\mathbf{A}_1$ (2.45 g, 79%). ^{1}H NMR ($CDCl_3$, 400 MHz, δ): 7.77 (d, 2H), 7.41 (d, 2H), 6.72 (d, 2H), 2.89 (t, 4H), 1.75 (t, 6H), 1.40–1.25 (m, 10H), 0.90 (m, 6H). ^{13}C NMR ($CDCl_3$, 400 MHz, δ): 152.09, 147.22, 138.48, 138.30, 132.57, 130.36, 124.96, 122.87, 31.56, 31.25, 30.46, 28.87, 22.59, 14.09. ^{1}H NMR and ^{13}C NMR spectra of the compound $\mathbf{A}_1$ with the assignment of the NMR signals were given in Figures S2 and S3 (Supporting Information), respectively. MALDI-TOF-MS *m/z*: $[M]^+$ calcd for $C_{28}H_{34}Br_2N_2S_2$, 620; found, 621.1.

2.6. Synthesis of the Polymer

The monomer $\mathbf{A}_1$ and BDT (0.4 mmol of each) were dissolved in degassed toluene (9 mL) in a 25 mL two-necked round-bottom flask. $Pd(PPh_3)_4$ (0.028 g, 6 mol%) was added, then the reaction mixture was stirred at 110 °C under argon atmosphere for 20 h. The polymer was then precipitated in a solution of methanol, filtered, and washed on a Soxhlet apparatus with methanol, hexane, and chloroform. The chloroform fraction was evaporated under reduced pressure, and the polymer was precipitated in methanol, filtered, and finally dried under high vacuum. The polymer **PBDT-DTQx** can be easily dissolved in commonly used solvents, like chloroform, toluene, chlorobenzene, etc. The molecular weight of **PBDT-DTQx** was measured by GPC with $\bar{M}_w$ = 14.6 kDa and PDI = 1.71. ^{1}H NMR ($CDCl_3$, 400 MHz, δ): 8.49–8.40 (m, 2H), 8.18–8.04 (m, 2H), 7.64–7.40 (m, 4H), 6.99–6.91 (m, 2H), 6.70 (m, 2H), 2.92 (m, 8H), 1.80 (m, 8H), 1.38–1.35 (m, 20H), 0.93–0.83 (m, 12H).

3. Results and Discussion

3.1. Thermal Properties

The thermal stability of the copolymer was investigated with TGA under a nitrogen atmosphere, as shown in Figure 1. The onset temperature with 5% weight-loss (T_d) of **PBDT-DTQx** is 306 °C, which is also listed in Table 1. Obviously, the thermal stability of the copolymer is adequate for their application in PSCs and other optoelectronic devices.

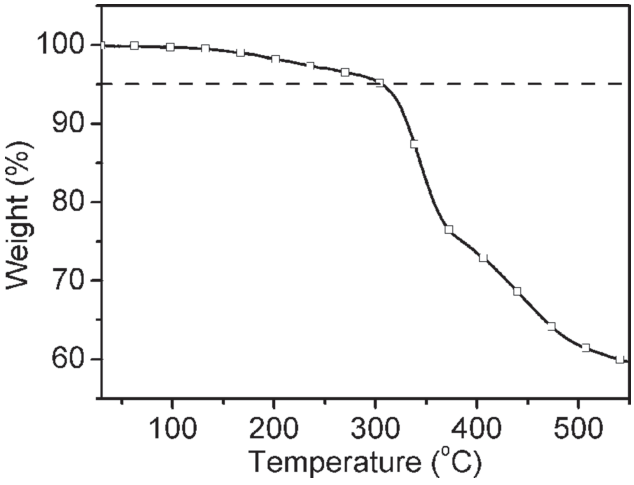

Figure 1. TGA plot of **PBDT-DTQx** with a heating rate of 10 °C min^{-1} under the nitrogen atmosphere.

3.2. Optical Properties

Figure 2 shows the UV–vis absorption spectra of **PBDT-DTQx** in dilute $CHCl_3$ solution and in the solid film on quartz plate. The film and solution absorption of **PBDT-DTQx** display similar absorption band (see Figure 2). While the maximal absorption peak of **PBDT-DTQx** film is red shifted by 53 nm compared with that of its solution, which reveals stronger intermolecular π–π interaction existing in the **PBDT-DTQx** film, which is beneficial to higher charge-carrier mobility. The absorption edges of **PBDT-DTQx** film are located at 723 nm (see Table 1), corresponding to an optical bandgap (E_g^{opt}) of 1.72 eV.

3.3. Electrochemical Properties

Electrochemical cyclic voltammetry has been widely employed to investigate the electrochemical behavior of the conjugated polymers and estimate its HOMO and LUMO energy levels. The HOMO and LUMO energy levels of the polymer were calculated from the onset oxidation potential (ϕ_{ox}) and onset reduction potential (ϕ_{red}) according to the following equations: $E_{HOMO} = -e(\phi_{ox} + 4.4)$ (eV) and $E_{LUMO} = -e(\phi_{red} + 4.4)$ (eV), where the unit of potential is V versus Ag/AgCl. As shown in the cyclic voltammogram

Table 1. Thermal and physical properties of **PBDT-DTQx.**

T_d[a)] [°C]	λ_{edg}[b)] [nm]	E_g^{opt}[c)] [eV]	ϕ_{ox} [V]	ϕ_{red} [V]	HOMO[d)] [eV]	LUMO[d)] [eV]
306	723	1.72	0.95	–0.80	–5.35	–3.60

[a)]5% weight loss temperature measured by TGA under N_2; [b)]For the polymer film; [c)]Bandgap, estimated from the optical absorption band edge of the film; [d)]Calculated from the onset oxidation and reduction potentials of the polymer.

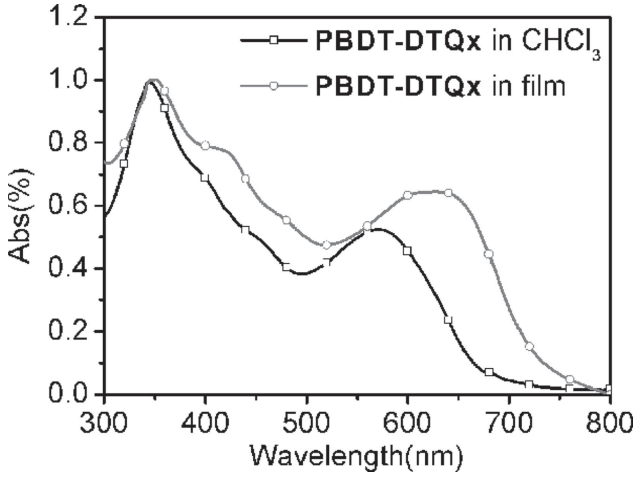

Figure 2. UV–vis absorption spectra of **PBDT-DTQx** in $CHCl_3$ solution and solid film spin-coated on quartz plate.

of **PBDT-DTQx** in Figure 3, the φ_{red} is –0.80 V versus Ag/AgCl, and the ϕ_{ox} is 0.95 V versus Ag/AgCl. Thus, the HOMO and LUMO energy levels as well as the electrochemical bandgap (E_g^{EC}) of the polymer **PBDT-DTQx** are –5.35, –3.60, and 1.75 eV, respectively. The E_g^{EC} agrees well with the E_g^{opt}. Compared with some of the **Qx**-relevant D–A copolymers reported in the literature,[10,11,13c] the lower HOMO energy levels of **PBDT-DTQx** are beneficial to a higher open-circuit voltage (V_{oc}) for the PSCs with the polymer as donor because V_{oc} of PSCs is related to the difference of the LUMO of the acceptor and the HOMO of the donor materials.

3.4. Photovoltaic Properties

PSCs were fabricated from **PBDT-DTQx** as donor and (6,6)-phenyl-C_{61}-butyric acid methyl ester ($PC_{60}BM$) or

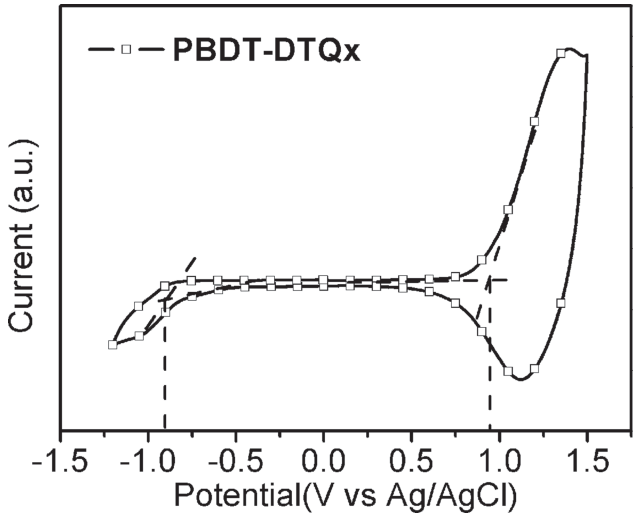

Figure 3. Cyclic voltammogram of **PBDT-DTQx** film on glassy carbon electrode in a 0.1 mol L^{-1} n-Bu_4NPF_6 acetonitrile solution at a scan rate of 100 mV s^{-1}.

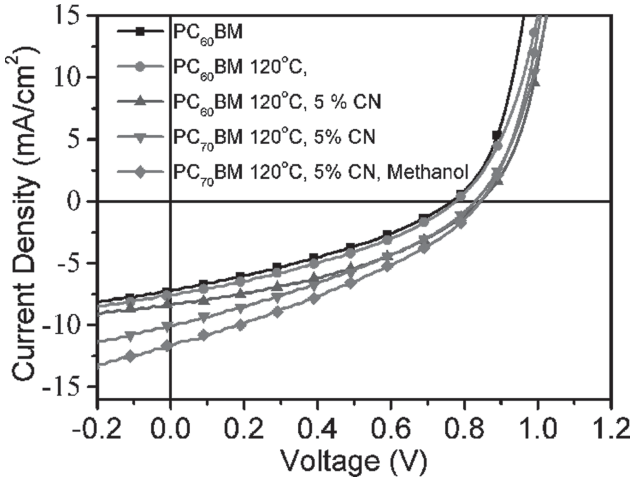

Figure 4. *J–V* curves of the PSCs based on **PBDT-DTQx** as donor and $PC_{60}BM$ or $PC_{70}BM$ as acceptor with the donor/acceptor weight ratio of 1:2.5 with different processing conditions under the illumination of AM 1.5, 100 mW cm^{-2}.

(6,6)-phenyl-C_{71}-butyric acid methyl ester ($PC_{70}BM$) as acceptor. Figure 4 shows the current density–voltage (*J–V*) curves of the PSCs based on **PBDT-DTQx**/$PC_{60}BM$ or **PBDT-DTQx**/$PC_{70}BM$ with different processing conditions, under the illumination of AM 1.5, 100 mW cm^{-2}. The photovoltaic performance data of the PSCs, including the V_{oc}, short-circuit current density (J_{sc}), fill factor (FF), and PCE values, are summarized in Table 2 for a clear comparison. In the optimization of the donor/acceptor weight ratio in the PSCs based on **PBDT-DTQx**/$PC_{60}BM$, the weight ratio of 1:2.5 with thermal annealing at 120 °C for 10 min gave the best photovoltaic performance with a PCE of 2.06%.

Solution additive has been proven to be an effective approach to improve the interpenetrating network morphology of the active layer and photovoltaic performance of the PSCs.[17–21] In order to further improve PCE of the PSCs, we choose CN and DIO as solvent additive. We found the device based on **PBDT-DTQx**:$PC_{70}BM$ (1:2.5, w/w) with 5% CN additive displayed an optimal PCE of 2.73% with a

Table 2. Photovoltaic properties of the PSCs based on **PBDT-DTQx**/$PC_{60}BM$ with different D/A weight ratios, under the illumination of AM 1.5, 100 mW cm^{-2}.

Blend ratio	V_{oc} [V]	J_{sc} [mA cm^{-2}]	FF	PCE [%]
1:1	0.75	5.98	0.33	1.48
1:2	0.76	7.07	0.32	1.72
1:3	0.77	6.42	0.34	1.68
1:2.5	0.77	7.24	0.33	1.84
1:2.5[a)]	0.78	7.58	0.35	2.06

[a)]With thermal annealing at 120 °C for 10 min.

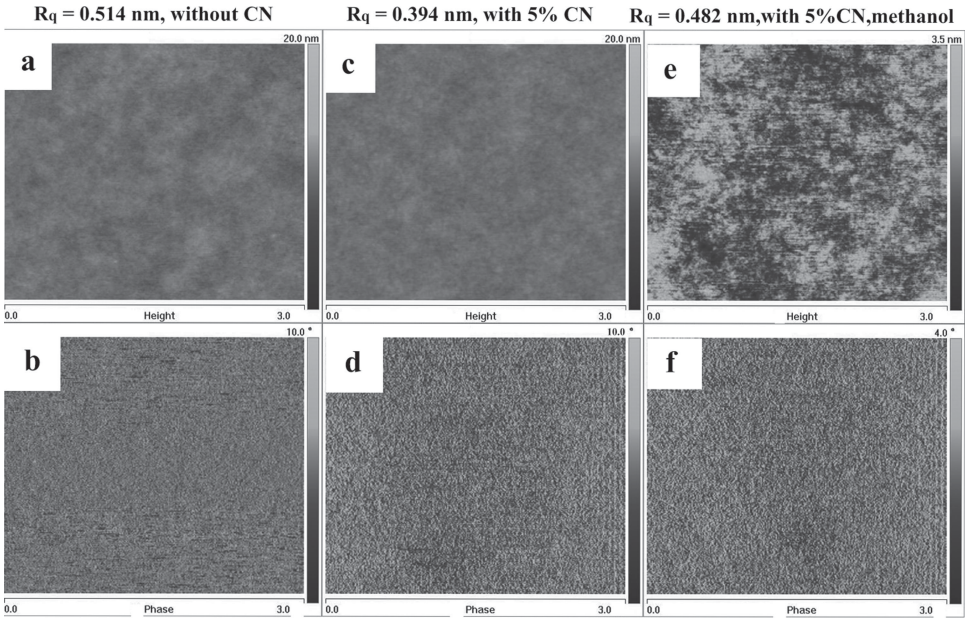

Figure 5. Tapping-mode AFM: (top) topography image, (bottom) phase image of the blend films of **PBDT-DTQx**/$PC_{70}BM$ (1:2.5, w/w) after thermal annealing at 120 °C for 10 min. a,b): without CN; c,d): with 5% CN; e,f): with 5% CN and methanol treatment after thermal annealing.

V_{oc} of 0.84 V, a J_{sc} of 8.35 mA cm^{-2}, and a FF of 0.39. When $PC_{70}BM$ was used as acceptor, an enhanced PCE of 3.15% with a higher J_{sc} of 10.10 mA cm^{-2} was achieved, due to the stronger absorption of $PC_{70}BM$ in the visible region in comparison with $PC_{60}BM$. Figure 5a,d shows atomic force microscopy (AFM) images of the active layer of the PSCs at different fabrication conditions. From the topography images (Figure 5a,c), the mean-square surface roughness (R_q) of blend films with and without CN additive is 0.394 and 0.514 nm, respectively, which means that more smooth film morphology was formed with CN additive compared with the blend film without CN additive. The phase images in Figure 5b,d indicate that the interpenetrating network in the active layer of the PSCs was improved with CN additive.

Recent studies have shown that the device performance of PSCs could be significantly enhanced by treatment with polar solvents.[2e,22,23] In this study, we choose methanol[24] as typical treatment solvent because it has been widely used in the surface engineering. A higher PCE of 3.90% was achieved in the optimized devices with methanol treatment after thermal annealing. For comparison, the data were listed in Table 3. Methanol treatment leads to a significant 23.8% enhancement in PCE with a simultaneous improvement in V_{oc} (0.82–0.83 V), J_{sc} (10.10–11.71 mA cm^{-2}), and FF (0.38–0.40).

Table 3. Photovoltaic properties of the PSCs based on **PBDT-DTQx** as donor and $PC_{60}BM$ or $PC_{70}BM$ as acceptor (1:2.5, w/w) with different processing conditions and with thermal annealing at 120 °C for 10 min, under the illumination of AM 1.5, 100 mW cm^{-2}.

Acceptor	With CN	With DIO	V_{oc} [V]	J_{sc} [mA cm^{-2}]	FF	PCE [%]
$PC_{60}BM$	1%	No	0.75	6.30	0.33	1.56
	3%	No	0.79	6.61	0.35	1.83
	5%	No	0.84	8.35	0.39	2.73
	No	1%	0.74	5.65	0.37	1.54
	No	3%	0.74	6.35	0.34	1.60
	No	5%	0.78	6.11	0.33	1.57
$PC_{70}BM$	5%	No	0.82	10.10	0.38	3.15
	5%	No	0.83	11.71	0.40	3.90[a)]

[a)]Methanol treatment after thermal annealing.

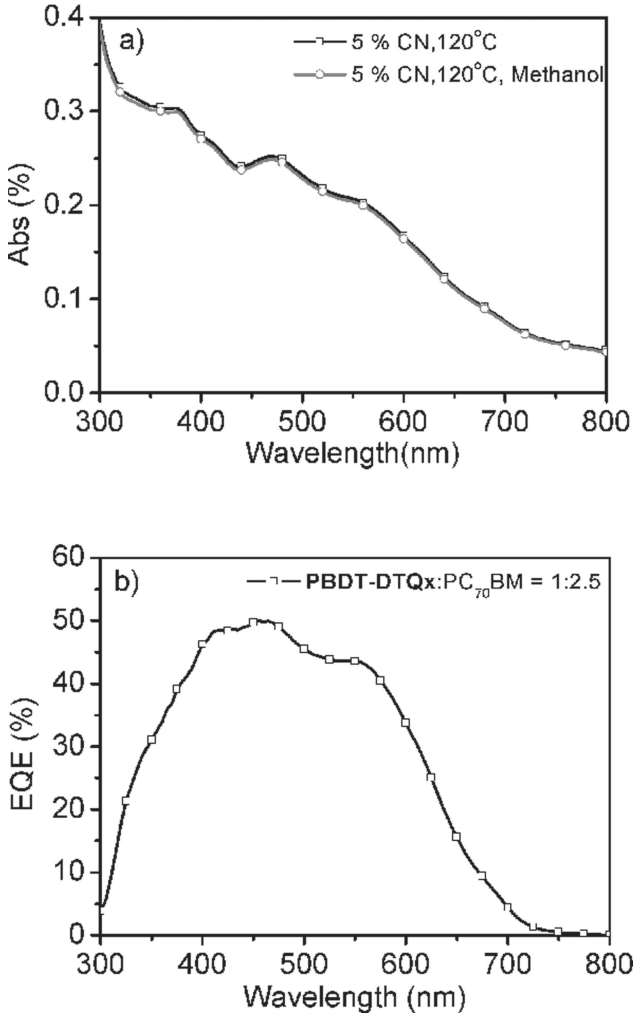

Figure 6. a) UV–vis absorption of the blend film of **PBDT-DTQx**:$PC_{70}BM$ with weight ratios 1:2.5 under different process; b) EQE spectra of the PSCs based on a **PBDT-DTQx**:$PC_{70}BM$ (1:2.5, w/w) blend film with CN as the additive and methanol treatment after thermal annealing.

In order to further investigate the influence of methanol treatment on surface morphology of the **PBDT-DTQx**:$PC_{70}BM$ blend film, we measured the AFM images of the blend films with methanol treatment, as shown in Figure 5e,f. From the topography image (Figure 5e), the R_q values are 0.482 nm for the blend film, and the phase image in Figure 5f clearly displays donor/acceptor interpenetrating networks in the film with methanol treatment, which should be beneficial to the improvement of the photovoltaic performance of the PSCs.[25]

Figure 6a shows absorption spectra of the blend films with or without methanol treatment. The blend film shows a broad absorption wavelength range from 300 to 700 nm. It is also worth noting that no obvious change was observed in the absorption spectrum of the blend film after methanol treatment. The results indicate there is no evident reconstruction of the surface of **PBDT-DTQx**:$PC_{70}BM$ blends after methanol treatment.[22,24a]

The external quantum efficiency (EQE) spectrum of the device with the optimized fabrication condition was shown in Figure 6b. The **PBDT-DTQx**:$PC_{70}BM$ blend film showed a higher EQE value of over 40% with a fairly broad response range (400–600 nm), which is consistent with the higher J_{sc} of the corresponding PSCs.

4. Conclusion

A new D–A copolymer **PBDT-DTQx** based on 2,3-di(5-hexylthiophen-2-yl)quinoxaline acceptor unit and BDT donor unit was designed and synthesized. With the optimization of CN additive, the device based on **PBDT-DTQx**:$PC_{70}BM$ (1:2.5, w/w) displayed a PCE of 3.15% with a V_{oc} of 0.82 V, a J_{sc} of 10.10 mA cm^{-2}, and a FF of 0.38. After methanol treatment, a significant 23.8% enhancement in PCE (up to 3.90%) was achieved with a simultaneous improvement in V_{oc} (0.82–0.83 V), J_{sc} (10.10–11.71 mA cm^{-2}), and FF (0.38–0.40). The results indicate that **PBDT-DTQx** is a promising polymer-donor material for further application in efficient PSCs.

Supporting Information

Supporting Information is available from the Wiley Online Library or from the author.

Acknowledgements: This work was supported by the Ministry of Science and Technology of China (2014CB643501 and 2011AA050523) and NSFC (91333204 and 51203168).

Received: December 26, 2013; Revised: January 19, 2014; Published online: February 25, 2014; DOI: 10.1002/macp.201300793

Keywords: conjugated D–A copolymers; polymer solar cells; quinoxaline acceptor unit

[1] G. Yu, J. Gao, J. C. Hummelen, F. Wudl, A. J. Heeger, *Science* **1995**, *270*, 1789.
[2] a) K. Li, Z. Li, K. Feng, X. Xu, L. Wang, Q. Peng, *J. Am. Chem. Soc.* **2013**, *135*, 13549; b) M. Zhang, Y. Gu, X. Guo, F. Liu, S. Zhang, L. Huo, T. P. Russell, J. Hou, *Adv. Mater.* **2013**, *25*, 4944; c) Z. He, C. Zhong, S. Su, M. Xu, H. Wu, Y. Cao, *Nat. Photonics* **2012**, *6*, 591; d) X. Li, W. C. H. Choy, L. Huo, F. Xie, W. E. I. Sha, B. Ding, X. Guo, Y. Li, J. Hou, J. You, Y. Yang, *Adv. Mater.* **2012**, *24*, 3046; e) Z. He, C. Zhong, X. Huang, W.-Y. Wong, H. Wu, L. Chen, S. Su, Y. Cao, *Adv. Mater.* **2011**, *23*, 4636.
[3] a) C. Cabanetos, A. E. Labban, J. A. Bartelt, J. D. Douglas, W. R. Mateker, J. M. J. Fréchet, M. D. McGehee, P. M. Beaujuge, *J. Am. Chem. Soc.* **2013**, *135*, 4656; b) K. H. Hendriks, G. H. L. Heintges, V. S. Gevaerts, M. M. Wienk, R. A. J. Janssen, *Angew. Chem Int. Ed.* **2013**, *52*, 8341; c) L. Dou, C.-C. Chen, K. Yoshimura, K. Ohya, W.-H. Chang, J. Gao, Y. Liu, E. Richard,

Y. Yang, *Macromol.* **2013**, *46*, 3384; d) I. Osaka, T. Kakara, N. Takemura, T. Koganezawa, K. Takimiya, *J. Am. Chem. Soc.* **2013**, *135*, 8834; e) T. Yang, M. Wang, C. Duan, X. Hu, L. Huang, J. Peng, F. Huang, X. Gong, *Energy Environ. Sci.* **2012**, *5*, 8208.

[4] J. You, L. Dou, K. Yoshimura, T. Kato, K. Ohya, T. Moriarty, K. Emery, C.-C. Chen, J. Gao, G. Li, Y. Yang, *Nat. Commun.* **2013**, *4*, 1446.

[5] a) Y. F. Li, *Acc. Chem. Res.* **2012**, *45*, 723; b) Y. F. Li, *Chem. Asian J.* **2013**, *8*, 2316; c) Y. J. He, Y. F. Li, *Phys. Chem. Chem. Phys.* **2011**, *13*, 1970; d) Y. J. He, H.-Y. Chen, J. H. Hou, Y. F. Li, *J. Am. Chem. Soc.* **2010**, *132*, 1377; e) Y. J. He, G. J. Zhao, B. Peng, Y. F. Li, *Adv. Funct. Mater.* **2010**, *20*, 3383.

[6] a) H. Zhou, L. Yang, W. You, *Macromolecules* **2012**, *45*, 607; b) A. C. Stuart, J. R. Tumbleston, H. Zhou, W. Li, S. Liu, H. Ade, W. You, *J. Am. Chem. Soc.* **2013**, *135*, 1806; c) L. Dou, W.-H. Chang, J. Gao, C.-C. Chen, J. You, Y. Yang, *Adv. Mater.* **2013**, *25*, 825; d) J.-M. Jiang, M.-C. Yuan, K. Dinakaran, A. Hariharan, K. H. Wei, *J. Mater. Chem. A* **2013**, *1*, 4415; e) D. Gendron, M. Leclerc, *Energy Environ. Sci.* **2011**, *4*, 1225.

[7] a) H. Son, L. Lu, W. Chen, T. Xu, T. Zheng, B. Carsten, J. Strzalka, S. B. Darling, L. X. Chen, L. Yu, *Adv. Mater.* **2013**, *25*, 838; b) X. Guo, N. Zhou, S. J. Lou, J. W. Hennek, R. P. Ortiz, M. R. Butler, P.-L. T. Boudreault, J. Strzalka, P.-O. Morin, M. Leclerc, J. T. L. Navarrete, M. A. Ratner, L. X. Chen, R. P. H. Chang, A. Facchetti, T. J. Marks, *J. Am. Chem. Soc.* **2012**, *134*, 18427; c) J. Liu, B. Walker, A. Tamayo, Y. Zhang, T.-Q. Nguyen, *Adv. Funct. Mater.* **2013**, *23*, 47; d) C. J. Brabec, M. Heeney, I. McCulloch, J. Nelson, *Chem. Soc. Rev.* **2011**, *40*, 1185.

[8] a) J. Hou, M.-H. Park, S. Zhang, Y. Yao, L.-M. Chen, J.-H. Li, Y. Yang, *Macromolecules* **2008**, *41*, 6012; b) L. Huo, J. Hou, S. Zhang, H.-Y. Chen, Y. Yang, *Angew. Chem Int. Ed.* **2010**, *49*, 1500; c) L. Huo, J. Hou, *Polym. Chem.* **2011**, *2*, 2453; d) C. Cui, J. Min, C.-L. Ho, T. Ameri, P. Yang, J. Zhao, C. J. Brabec, W.-Y. Wong, *Chem. Commun.* **2013**, *49*, 4409.

[9] a) C. Kitamura, S. Tanaka, Y. Yamashita, *Chem. Mater.* **1996**, *8*, 570; b) M. J. Edelmann, J.-M. Raimundo, N. F. Utesch, F. Á. Diederich, C. Boudon, J.-P. Gisselbrecht, M. Gross, *Helv. Chim. Acta* **2002**, *85*, 2195; c) A. Tsami, T. W. Bünnagel, T. Farrell, M. Scharber, S. A. Choulis, C. J. Brabec, U. Scherf, *J. Mater. Chem.* **2007**, *17*, 1353.

[10] a) R. Duan, L. Ye, X. Guo, Y. Huang, P. Wang, S. Zhang, J. Zhang, L. Huo, J. Hou, *Macromolecules* **2012**, *45*, 3032; b) Y. Huang, M. Zhang, L. Ye, X. Guo, C. C. Han, Y. Li, J. Hou, *J. Mater. Chem.* **2012**, *22*, 5700.

[11] a) C.-H. Chen, C.-H. Hsieh, M. Dubosc, Y.-J. Cheng, C.-S. Hsu, *Macromolecules* **2010**, *43*, 697; b) A. V. Patil, W.-H. Lee, E. Lee, K. Kim, I.-N. Kang, S.-H. Lee, *Macromolecules* **2011**, *44*, 1238; c) S. K. Lee, W.-H. Lee, J. M. Cho, S. J. Park, J.-U. Park, W. S. Shin, J.-C. Lee, I.-N. Kang, S.-J. Moon, *Macromolecules* **2011**, *44*, 5994.

[12] a) D. Kitazawa, N. Watanabe, S. Yamamoto, J. Tsukamoto, t*Appl. Phys. Lett.* **2009**, *95*, 053701; b) Y. Zhang, J. Zou, H.-L. Yip, K.-S. Chen, D. F. Zeigler, Y. Sun, A. K.-Y. Jen, *Chem. Mater.* **2011**, *23*, 2289; c) E. Wang, L. Hou, Z. Wang, Z. Ma, S. Hellström, W. Zhuang, F. Zhang, O. Inganäs, M. R. Andersson, *Macromolecules* **2011**, *44*, 2067; d) E. Zhou, J. Cong, K. Tajima, K. Hashimoto, *Chem. Mater.* **2010**, *22*, 4890; e) L. J. Lindgren, F. Zhang, M. Andersson, S. Barrau, S. Hellström, W. Mammo, E. Perzon, O. Inganäs, M. R. Andersson, *Chem. Mater.* **2009**, *21*, 3491.

[13] a) E. Wang, L. Hou, Z. Wang, S. Hellström, F. Zhang, O. Inganäs, M. R. Andersson, *Adv. Mater.* **2010**, *22*, 5240; b) X. Guo, M. Zhang, J. Tan, S. Zhang, L. Huo, W. Hu, Y. Li, J. Hou, *Adv. Mater.* **2012**, *24*, 6536; c) H.-C. Chen, Y.-H. Chen, C.-C. Liu, Y.-C. Chien, S.-W Chou, P.-T. Chou, *Chem. Mater.* **2012**, *24*, 4766.

[14] J. Zhang, W. Cai, F. Huang, E. Wang, C. Zhong, S. Liu, M. Wang, C. Duan, T. Yang, Y. Cao, *Macromolecules* **2011**, *44*, 894.

[15] A. Gadisa, W. Mammo, L. M. Andersson, S. Admassie, F. Zhang, M. R. Andersson, O. Inganäs, *Adv. Funct. Mater.* **2007**, *17*, 3836.

[16] F. Babudri, V. Fiandanese, G. Marchese, A. Punzi, *Tetrahedron Lett.* **1995**, *36*, 7305.

[17] F.-C. Chen, H.-C. Tseng, C.-J. Ko, *Appl. Phys. Lett.* **2008**, *92*, 103316.

[18] J. K. Lee, W. L. Ma, C. J. Brabec, J. Yuen, J. S. Moon, J. Y. Kim, K. Lee, G. C. Bazan, A. J. Heeger, *J. Am. Chem. Soc.* **2008**, *130*, 3619.

[19] K. R. Graham, P. M. Wieruszewski, R. Stalder, M. J. Hartel, J. Mei, F. So, J. R. Reynolds, *Adv. Funct. Mater.* **2012**, *22*, 4801.

[20] H. Xin, X. Guo, G. Ren, M. D. Watson, S. A. Jenekhe, *Adv. Energy Mater.* **2012**, *2*, 575.

[21] J. Peet, J. Y. Kim, N. E. Coates, W. L. Ma, D. Moses, A. J. Heeger, G. C. Bazan, *Nat. Mater.* **2007**, *6*, 497.

[22] X. Liu, W. Wen, G. C. Bazan, *Adv. Mater.* **2012**, *24*, 4505.

[23] Y.-M. Chang, R. Zhu, E. Richard, C.-C. Chen, G. Li, Y. Yang, *Adv. Funct. Mater.* **2012**, *22*, 3284.

[24] a) H. Q. Zhou, Y. Zhang, J. Seifter, S. D. Collins, C. Luo, G. C. Bazan, T.-Q. Nguyen, A. J. Heeger, *Adv. Mater.* **2013**, *25*, 1646; b) L. Ye, Y. Jing, X. Guo, H. Sun, S. Q. Zhang, M. J. Zhang, L. J. Huo, J. H. Hou, *J. Phys. Chem. C* **2013**, *117*, 14920.

[25] G. Li, V. Shrotriya, J. Huang, Y. Yao, T. Moriarty, K. Emery, Y. Yang, *Nat. Mater.* **2005**, *4*, 864.